Paper ID ILASS08-1-13

ILASS 2008
Sep. 8-10,2008, Como Lake, Italy

VALIDATION OF A CAVITATION AND TURBULENCE INDUCED MODEL FOR THE PRIMARY BREAKUP OF DIESEL JETS

Oscar J. Soriano[1]*, Martin Sommerfeld[2], Axel Burkhardt[1]

[1]Diesel Systems, Hydraulic Simulation, Continental Automotive GmbH, Regensburg, Germany
[2]Dept. of Process Engineering, Martin-Luther University Halle-Wittenberg,
Haale (Saale), Germany

ABSTRACT

In this paper, the performance of an energy based CFD model for the primary breakup of high-pressure Diesel jets is presented. This version of the model was modified and further developed for different turbulent and cavitating flow conditions experimentally found inside the injection hole. A detailed spatial and temporal resolution of the cavitating flow in the hole is used by the model to deliver three dimensional sprays, providing all the starting conditions for the calculation of the secondary breakup of the Diesel spray by means of a Lagrangian approach. The characteristic feature of the model is the variable size and velocity distribution of the primary droplets as a function of the available breakup energy. Other main advantage of the model is the direct calculation of the droplet size distribution and spray angle on the basis of the flow properties, so that empirical correlations or measurement data are not needed as input for the calculations. The two-fluid Eulerian simulation for the cavitating flow inside the nozzle is followed by an Eulerian / Lagrangian approach outside the nozzle, using the Ansys-CFX CFD code for both stages of the process. Measurements carried out in the test facilities of the Continental Automotive GmbH in Regensburg for high pressure Diesel jets were taken to compare with the simulations, offering satisfactory performance.

INTRODUCTION

Combustion in a direct injection engine is strongly controlled by the details of the atomized fuel spray produced by the nozzle in the injector, so that an understanding of this high-pressure sprays is central to the goal of optimizing fuel consumption in the development of new engines. Not only new developed experimental techniques can help reach this goal, but also computational methods show great potential for the characterization of these sprays.

The fundamental mechanisms of atomization have been under extensive experimental and theoretical study for many years [13, 6, 7]. Today it is accepted, that the breakup of liquid jets under high-pressure injection conditions can be divided in two sub-processes depending on the origin of the driving physical phenomena: primary and secondary breakup [3, 14]. In the case of primary breakup it is assumed that the main mechanisms that lead to the first breakup of the coherent liquid column into big liquid drops and ligaments can be found inside the injection nozzle. The most cited mechanisms found in the literature are cavitation and turbulence [5, 3, 6]. These are caused by the big pressure differences (up to 2000 bar) and the tiny geometrical dimensions of the nozzle ($D = 150\mu m$), which lead to very high velocities and low static pressures, locally under saturation pressure of Diesel. Cavitation structures develop because of the drop of static pressure inside the nozzle: the strong acceleration of the liquid at the inlet of the injection holes together with an additional radial pressure gradient caused by the strong curvature of the streamlines lead to a pressure fall below vapour pressure. The cavitation structures implode when entering the chamber because of the high ambient pressure. This energy contributes to the primary breakup and results in the formation of big droplets or fluid ligaments and also in spray divergence. Other cavitation structures implode inside the injection hole, increasing the turbulence level and promoting the spray disintegration into big droplets. Different authors have tried to describe the influence of turbulence and cavitation on the primary breakup [2, 11, 3, 17]. The further breakup of the primary drops and ligaments due to the aerodynamical interaction with the surrounding gas outside the nozzle is known as secondary breakup.

For the mathematical description of the spray and nozzle flow two approaches are used: the homogeneous (Euler/Euler) and the inhomogeneous (Euler/Lagrange) approach. The inhomogeneous approach does allow mass, momentum and energy exchange between the droplets and the gas phase, which is indispensable for Diesel spray calculations. Due to the easier implementation of the physical models and the robustness of the mathematical approach, a stochastic Lagrangian description of the Diesel spray is widely used in the literature, both for the secondary and primary breakup. According to this methodology, all processes, which cannot be resolved deterministic on a parcel level, are solved with a Monte-Carlo-simulation. This approach is in the case of secondary breakup extensively accepted, whereas for the primary some authors consider the homogeneous approach to be more efficient [18]. Regarding the nozzle flow simulations, almost in every literature reference the homogeneous approach is used, assuming the same velocity and pressure for both Diesel fuel and vapour.

While many models dealing with the secondary breakup can be

*Corresponding Author

found in the open literature (listed in [3]), very few have been developed to account for the important effects of the nozzle flow on the primary breakup. In the last few years a great effort is being made trying to describe the primary breakup, not without considerable difficulties. One of the main reasons for this is the different mathematical description of the liquid fuel inside and outside the injection nozzle, as explained above, that leads to a two-step simulation process of the fuel injection. Since the primary breakup of the liquid begins inside the nozzle but ends outside, the modelling of the breakup comprehends not only the acting physical processes, but also the change of mathematical approach.

SPECIFIC OBJECTIVES AND SIMULATION APPROACH

The objective of this paper is the validation of the performance of a cavitation and turbulence-induced break-up spray model by means of optical measurements of the penetration and angle of the injected spray. The initial turbulent and cavitating conditions of the spray are obtained from unsteady in-nozzle flow simulations of a two-hole real size injection nozzle.
The simulation approach comprehend the unsteady simulation of the nozzle flow, recording the spatial distribution of the flow properties $(\vec{v}, \rho, k, \epsilon)$ at the nozzle exit as a function of time, both for Diesel fuel and Diesel vapour. These properties are then used as a boundary condition for the subsequent unsteady Lagrangian spray calculations, yielding initial conditions for the spray velocities, injected mass and available breakup energy. The unsteady simulation of the nozzle flow was carried out including the movement of the needle (injector opening).

This coupling method is convenient to deal with the atomization of non-axial symmetric liquid jets penetrating in dense gaseous ambient with very high velocities like the ones encountered in high pressure Diesel injection. Under these conditions a very fast disintegration of the coherent liquid flowing in the nozzle into drops of different sizes and shapes can be expected. This assumption of a very short intact core length can be found quite often in the literature [14]. Thus, the present numerical transition of the Eulerian two-phase flow in the nozzle into the Lagrangian two-phase particle flow in the chamber should offer a good approach to the problem.
The performance of the primary breakup model is then evaluated by means of a comparison between the results of the spray simulations and optical spray measurements, including spray penetration $S_p(t)$, near and far spray angles. All measurements were carried out in the test facilities of Continental Automotive GmbH in Regensburg [9].

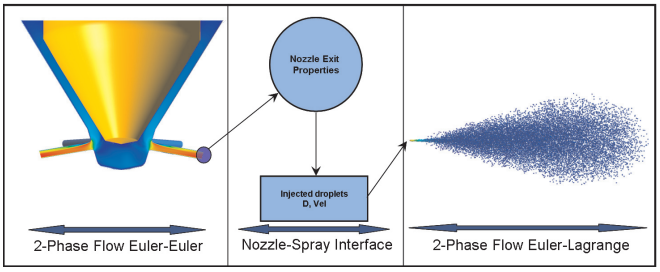

Figure 1: Simulation Approach

NOZZLE FLOW SIMULATION SETUP

The primary breakup model uses detailed information from 3D turbulent cavitating nozzle flow simulations performed with the Ansys CFX CFD code based on a Volume of Fluid (VOF) method [1]. This model was chosen because it offers a good compromise between computational effort and results quality. The VOF-model assumes that both gas and liquid phases share the same pressure and velocity. The two-phase flow is considered homogeneous, isothermal and the liquid and vapour phases incompressible, having constant density values. The calculations are time-dependent because of the highly transient behaviour of the nozzle flow, specially in the needle opening phase.
The simplified Rayleigh-Plesset model is employed for the mass transfer term between phases. This model bases on the growth of a single spherical bubble in an unbounded liquid domain [4]. The SST shear stress transport turbulence model is employed in the simulations [1], assuming the flow to be fully turbulent. Fluid temperature is assumed to be constant in the whole domain and the energy equation is not solved.
For the nozzle simulations meshes of about 10^6 cells were used, paying special attention on the resolution of the boundary layer with 8-10 nodes. The movement of the needle is simulated with the Displacement Diffusion model [1]. With this model, the displacement applied on the needle is diffused to other mesh points by solving the equation:

$$\nabla \cdot (\Gamma_{disp} \nabla \delta) = 0 \tag{1}$$

In this equation, δ is the displacement relative to the previous mesh locations and Γ_{disp} is the mesh stiffness, which determines the degree to which regions of nodes move together.
Figure 2 shows the geometry of one of the injection holes of the studied nozzle. Both holes have different values of included angle, that is the angle included between the injector axis and the injection hole axis. Higher included angles show higher tendencies to cavitate and to produce an asymmetric flow inside the hole. The important geometrical parameters for this paper are listed on Table 2. Here, CF (conicity factor) and HE (inlet rounding) are typical geometrical parameters of Diesel injection nozzles [9], where

$$CF = \frac{D_{in} - D_{out}}{L_{hole}} \cdot 100 \tag{2}$$

Low values of CF and HE cause high curvature of the streamlines, promoting cavitation.

The duration of the simulations equals the typical injection time t_{inj} of $1ms$ using a timestep of $\Delta t = 1.5 \cdot 10^{-6} s$. The rest of the boundary conditions of the problem are summarised in Table 1. The operating points were chosen in order to appreciate the influence of both back (p_{geg}) and injection pressures (p_{vor}) on the calculated sprays.

VALIDATION OF NOZZLE FLOW

As a first step, the simulations of the cavitating flow are validated by comparing hydraulic flow measurements of the nozzles with the computed values. The measured hydraulic properties of the nozzle are the hydraulic flow, the characteristic curve and the critical cavitation point CCP, which are defined in the next paragraphs.

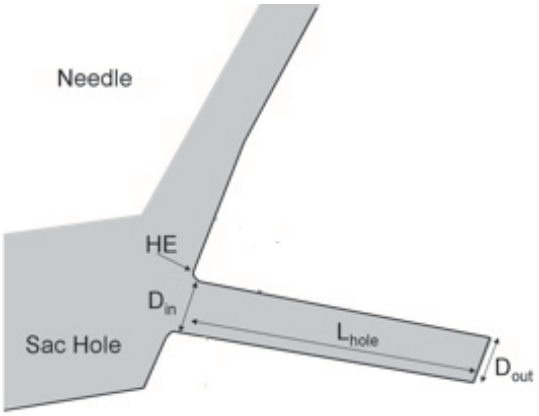

Figure 2: Scheme of nozze tip. Geometrical parameters

Case	p_{vor}	p_{geg}
1	800	20
2	1300	20
3	1600	10
4	1600	20
5	1600	40

Table 1: Operating points for experiments and simulations

Inj. Hole	$HE(\mu m)$	$HW(°)$	$CF(-)$
1	11	72	0.675
2	11	88	0.6

Table 2: Geometrical parameters of the studied nozzles

The nozzle *hydraulic flow* is the measured Diesel flow through a nozzle for a pressure difference of 100 bar. For a better evaluation of these results, the hydraulic flow of the nozzle is calculated under ideal conditions (Bernouilli equation) so that the efficiency of the nozzle can be described with a single parameter

$$\eta = \frac{HD}{HD_{ber}} \tag{3}$$

Hydraulic flow simulations show a good agreement, for the uncertainty of the hydraulic flow test bench is of about 3%.
The *characteristic curve* of the nozzle in Fig. 3 shows the

$\mathbf{HD_{ber}}$	$\mathbf{HD_{exp}}$	$\eta_{\mathbf{exp}}$	$\mathbf{HD_{sim}}$	$\eta_{\mathbf{sim}}$
$5.86 \cdot 10^{-3}$	$4.32 \cdot 10^{-3}$	**0.738**	$4.37 \cdot 10^{-3}$	**0.746**

Table 3: Hydraulic flow in l/s and efficiency of the studied nozzles

massflow of the nozzle for different needle lifts, under a driving pressure difference of $\Delta p = 100$ bar. It can be seen that the calculated hydraulic flow agrees quite well with the measured one. It is important to note that the nozzle reaches its nominal hydraulic flow for needle lifts higher than 50-60 μm. For lower lifts, the flow is determined by the gap between the needle and the seat area of the needle. It rises with the needle until the main throttle is shifted to the injection hole. This behaviour is well reproduced by the simulations.

For the characterisation of the cavitating conditions of the flow

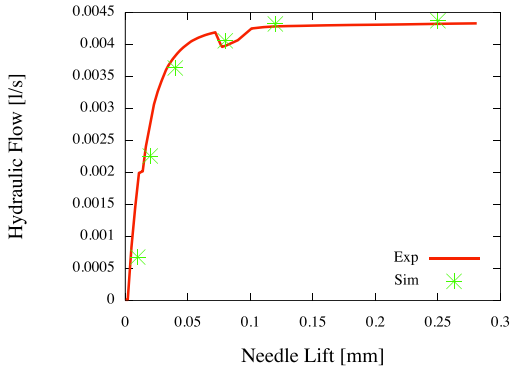

Figure 3: Characteristic curve of the investigated nozzle. Experiment and simulation.

the *critical cavitation point CCP* is of great help. The CCP is a non-destructive hydraulic measurement accounting for the relation of inj. pressure to back pressure for the onset of "choked flow" [9, 6]. To obtain this point, several measurements of the hydraulic flow are carried out for a constant injection pressure of $p_{vor} = 100$ bar while decreasing the back pressure from $p_{geg} = 100$ bar to $p_{geg} = 1$ bar. As seen in Figure 4, the simulated hydraulic flow of the nozzle increases with the pressure difference and the nozzle begins to cavitate so that a part of the flow cross section is filled with vapour. At a certain point the nozzle delivers a more or less constant hydraulic flow even if the pressure difference is raised. The point where the nozzle is "choked" because of cavitation is well reproduced by the simulation.

It is important to mention that turbulence was assumed to

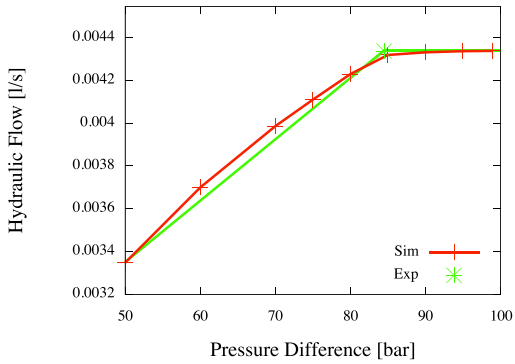

Figure 4: Determination of the CCP. Experiment and simulation.

be fully developed for all calculations. This is probably not true because of the length of the nozzle, which is not enough for turbulence to develop. From this point of view, the flow instabilities are overestimated by the calculations. At the same time, the collapse and detachment of vapour cavities inside the injection hole, which cause instabilities in the flow and promote the breakup, can't be calculated with the chosen mathematical approach. From this other point of view, the instabilities which promote breakup will be underestimated. It is assumed for this work that both effects are balanced and the general level of instabilities is well estimated.

After assuring the reliability of the simulations setup of the nozzle, unsteady simulations were carried out for the boundary

conditions shown in Table 1. The variables which play a role for the subsequent breakup of the liquid ($\vec{v}, \rho, k, \epsilon$) are then recorded as a function of time and space to be used as initial conditions by the primary breakup model.

PRIMARY BREAKUP MODEL

Based on the results of a detailed investigation of the flow inside the injection holes of high pressure Diesel injectors [5], a model for cavitation and turbulence induced primary break-up of liquid jets was developed some years ago [3]. The model uses a cavitation and turbulent energy based approach for the evaluation of all necessary starting conditions for the calculation of secondary break-up like drop sizes, velocity components and spray angle. This model has been now enhanced to be applied for 3D nozzle flow simulations accounting not only for turbulence and cavitation intensities inside the injection hole, but also for the velocity distribution at the hole exit.
The break-up energy is estimated by means of a two-phase flow simulation of the nozzle, as explained above. After that, an energy balance is drawn in order to calculate the properties of the primary injected droplets. The probability for new particles to be created at a certain position of the nozzle exit depends on the spatial resolution of the mass flow at the nozzle exit, so that a higher mass flow is represented by a higher number of particles. The spray angle is given by the diverging velocities described in the initial droplet velocity vectors $\vec{v}$. With this coupled approach, no initial value from empiric correlations needs to be used in the simulation chain and asymmetries of the nozzle flow are reproduced in the spray.
The break-up energy consists of the two following terms: flow-induced turbulent kinetic energy E_{turb} [3, 2] and cavitation induced turbulent kinetic energy E_{cav} [17, 3, 11]. Turbulent fluctuations acting on the surface of a jet cause instabilities which lead to break-up. The same approach is used when considering the instabilities caused when modeling the released energy of collapsing cavitation bubbles: only the induced instabilities near the surface are assumed to contribute to the break-up. Flow induced turbulent kinetic energy is a direct output of nozzle flow simulation, while cavitation induced turbulent kinetic energy has to be calculated by resolving the cavitation bubble dynamics [3].
As a first step, the flow at the nozzle exit is divided in two zones depending on the liquid and gas contents. Cells with a volume fraction of vapour $VF > 0.1$ belong to the cavitating zone (zone 2) and the rest to the liquid zone (zone 1), as seen in figure 5. Then, a cylindrical control volume for the energy balance is defined, where the length is equal to the effective diameter d_{eff} of the liquid zone. After that, the break-up energy is evaluated for each zone as follows:

$$E_i = \eta_i \cdot (E_{cav,i} + E_{kin,turb,i}) \tag{4}$$

Here, i=zone 1 or zone 2 and η represent the efficiency of the energy transformation, and has a value of 1 for this first evaluation of the model.
It is assumed that the total break-up energy in zone 2 turns into surface energy for the formation of n_2 droplets and for their radial kinetic energy.

$$E_{2,eff} = E_{\sigma 2} + E_{kin2} \tag{5}$$

$$E_{\sigma 2} = \sigma \cdot \pi d_{cav}^2 \cdot n_2 \tag{6}$$

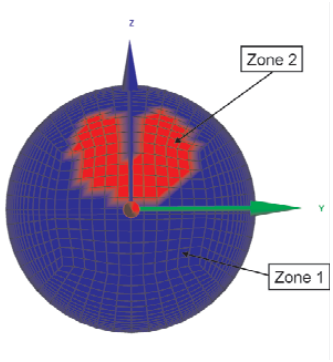

Figure 5: Typical distribution of zones at the nozzle exit

$$E_{kin2} = \frac{1}{2} \cdot v_{r2}^2 \cdot m_{droplet} \cdot n_2 \tag{7}$$

$$n_2 = \frac{6 \cdot m_2}{\pi \cdot d_{cav}^3 \cdot \rho_l} \tag{8}$$

For the liquid zone it is assumed that the total energy is present as turbulent fluctuations that act against the stabilizing surface forces [3, 11]. Mass is split off the liquid zone until both forces are in equilibrium:

$$U_{turb} = \sqrt{\frac{2 \cdot E_1}{3 \cdot m_1}} \tag{9}$$

$$F_{turb} = \frac{1}{2} \rho_L \cdot u_{turb}^2 \cdot S \tag{10}$$

$$F_\sigma = 2 \cdot \sigma \cdot (2 \cdot d_{eff}) \tag{11}$$

$$C \cdot F_{turb} = F_\sigma \tag{12}$$

Here, S is the surface of the liquid where the turbulent disrupting force is acting and d_{eff} the effective diameter of zone 1. In order to obtain plausible values for the diameter of the injected droplets it is necessary to multiply the disrupting force by a coefficient $C = O(10^{-2})$ [2].
The remaining mass is transformed to a cylindrical droplet of diameter $d_{rem,cyl}$, and its energy content is used to calculate its radial velocity.

$$d_{rem,cyl} = \frac{2 \cdot \sigma \cdot S/d_{eff}}{\frac{S/d_{eff} \cdot \rho_L \cdot E_1}{3 m_1} - 2\sigma} \tag{13}$$

The cylindrical droplet is then turned into a spherical one:

$$d_{rem} = \sqrt[3]{\frac{3}{2} \cdot d_{rem,cyl}^2 \cdot S/d_{eff}} \tag{14}$$

The split mass undergoes then the same calculation of eq 5 to eq 7 in order to obtain droplets of size d_{spl}.

SPRAY SIMULATION SETUP

For the description of the spray penetrating the dense gas ambient two phases are considered: the dispersed phase (fluid droplets) and the gas phase (continuum). The gas phase is modeled with the Eulerian approach using the Navier Stokes equations, while the dispersed phase is tracked through the flow in a Lagrangian way. The tracking is carried out by forming a set of ordinary differential equations in time for each particle, consisting of equations for position and velocity [15].

Since the concentration of the droplets in the fluid stream is high, two-way coupling is considered between the phases. This implies that the fluid affects the particle motion through the viscous drag and a difference in velocity between the particle and fluid, and conversely, there is a counteracting influence of the particle on the fluid flow due to the viscous drag. Droplet collision and coalescence are not considered. In addition to the drag forces, turbulent dispersion is also taken into account for these simulations. Although the gas-phase turbulence induced by this high-pressure-driven spray is anisotropic [12], an isotropic dispersion approach with the $k-\epsilon$ model is used. The initial turbulence levels are very low ($k = 1e^{-4}$ and $\mu_{turb} = 0.1$). For the secondary breakup, the Cascade Atomization Breakup model (CAB) was used [16] due to its good performance for high pressure Diesel sprays [10]. This model allows droplets to deform, so that a modification of the drag coefficient due to the variation of the droplet cross section is needed. The particle source terms are generated for each particle as they are tracked through the flow. Particle sources are applied in the control volume that the particle is in during the time step.

It is well known that the mesh can play an important role when simulating sprays with the Lagrangian approach. For this work an adaptive mesh was used (Fig. 6), so that for the perpendicular directions, the used lengths of a computational cell for the calculations are about 0.15 mm. in the dense spray zone and 0.8 mm. for far field of the spray. In the axial direction, an almost constant cell length of 0.8 mm. was used. The domain has a total length of 10 cm. in the axial direction and 2 cm. in the other two perpendicular directions., which results in a total number of cells of about 10^5. For all calculations a parcel injection rate of $2 \cdot 10^8$ parcels per second was taken, which should be enough to deliver statistical convergence for the calculation.

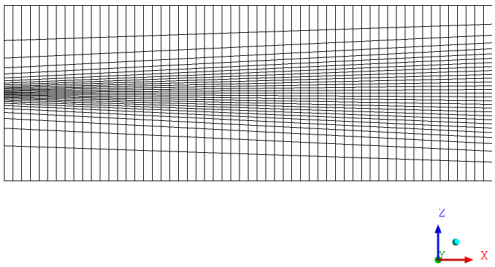

Figure 6: Mesh

VALIDATION OF SPRAY CALCULATIONS

Taking into account the limitations and sensitivities of the Lagrangian approach, the calculations are now compared to measurements. Due to the limited extension of this paper, the evaluation of the model performance will be carried out by means of the comparison of the sprays produced by only the injection hole 1, which is defined on Table 2. Due to the low values of HE and CF, cavitation and high turbulence values are expected, and confirmed with the validation of the nozzle flow (Fig. 4).

The spray visualization was performed using a CCD Camera and a backlight [9]. Spray penetration and both near and far spray angles were obtained as a function of time for the investigated sprays. The definition of the far spray angle and penetration can be obtained from Figure 7, where the mass of the spray is divided into three zones, containing 20%, 50% and 99% of the spray mass. The near field spray angle is defined

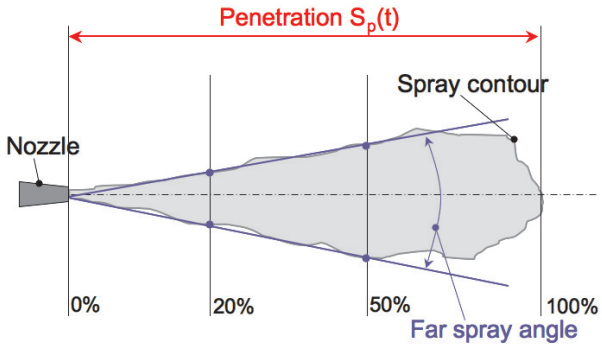

Figure 7: Definition of spray parameters

as the angle between the spray contour for 20% of the spray mass and the point of intersection between the injection hole axis and the injector axis.

In Figure 8a the influence of the injection pressure on the spray penetration is represented. As expected, higher pressure differences lead to a higher spray impulse, resulting in higher penetration. This tendency can be observed in the diagram, both for the computed and measured sprays. The agreement between experiments and simulations is good for the first half of the injection, which confirms that the nozzle simulations yield correct initial impulse conditions. For the second half of the injection, the penetration is underestimated due to both the lack of coalescence model in the CFD code and to the mesh sensitivity of the Lagrangian approach. The coalescence model in dense sprays would cause "old" slow droplets in spray to interact with "new" droplets, leading to higher droplet sizes and velocities which could penetrate further. The second reason is the mesh dependency of the Lagrangian approach: here the code underestimates the momentum exchange between phases so that the acceleration of the gas phase is lower than the real one and the spray is slowed down.

In Figure 8c the development in time of the mean size of the injected primary droplets, i.e. before secondary breakup, is represented together with the needle lift. For low needle lifts, the smallest flow cross section can be found in the needle seat area, and the flow in the injection holes is slow, not cavitating and laminar. Under these conditions, the available breakup energy is very low and therefore the injected droplets are big, of the size of the hole diameter. This corresponds to the well known and widely used "blob method" of Reitz et al. for the primary breakup [13]. If the needle continues to open, the flow is not restricted anymore in the needle seat area causing an acceleration of the flow in the injection hole. This results in an increase of available breakup energy, present in the flow as cavitating and turbulent instabilities, so that the model yields smaller droplets. These two Figures 8a and 8c show that the presented primary breakup model can reproduce the effect of a variation of the inj. pressure on the spray penetration and the droplet size distribution. As expected and often shown in the literature, in the case of a higher injection pressure the mean size of the droplets is smaller and the spray penetrates further, although the curves in the case of penetration show almost the same values. There are two counteracting effects on the penetration length when increasing the injection pressure. On one hand the impulse of the flow leaving the nozzle is higher,

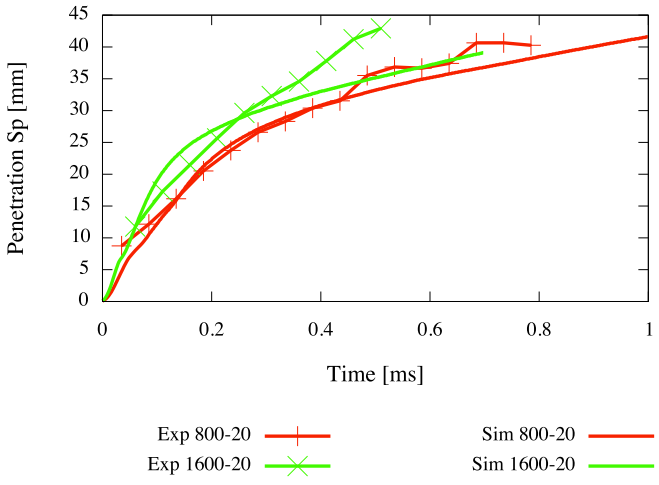

(a) Spray penetration for different injection pressures

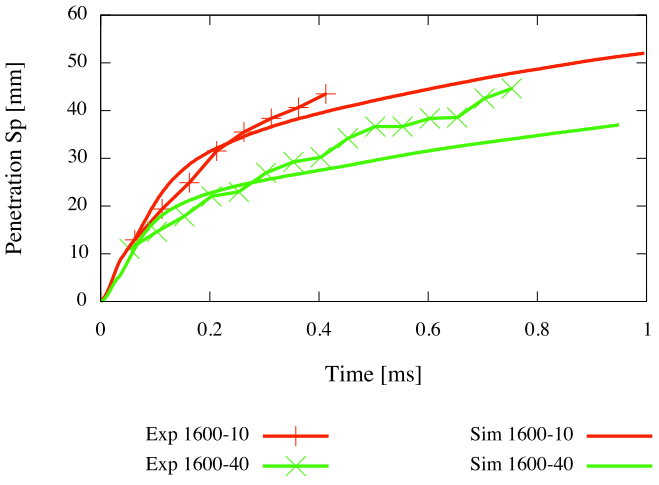

(b) Spray penetration for different back pressures

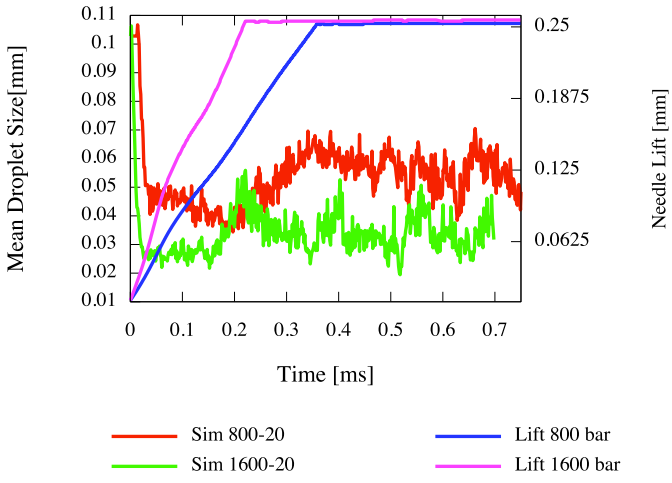

(c) Mean primary droplet sizes and needle lift. Variation of injection pressure

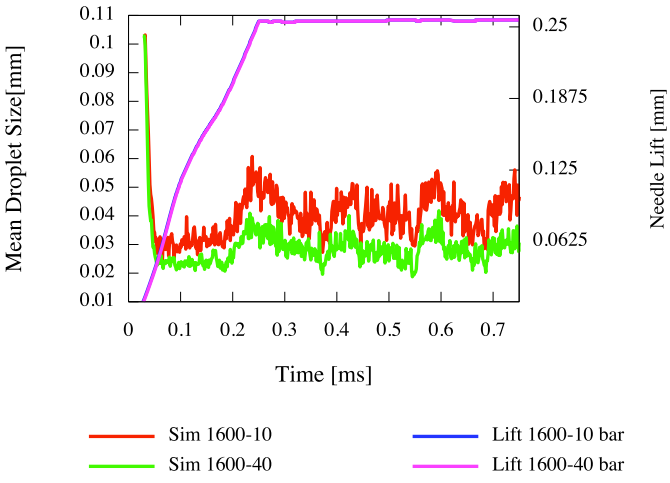

(d) Mean primary droplet sizes and needle lift. Variation of back pressure

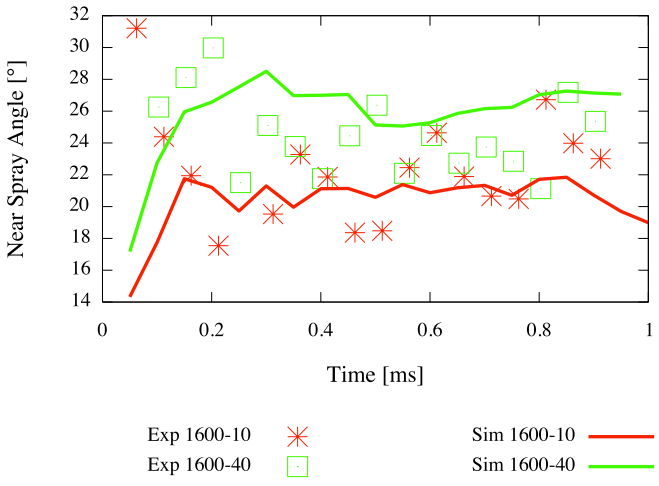

(e) Influence of back pressure on near spray angles

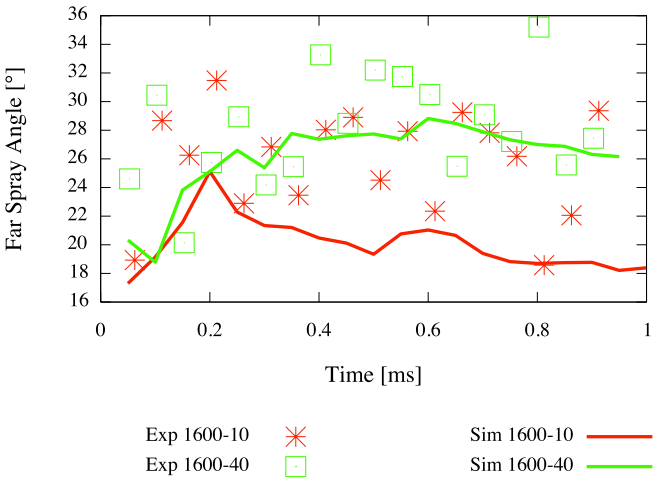

(f) Influence of back pressure on far spray angles

Figure 8: Simulation vs. experimental results

which leads to higher penetration, but on the other hand the droplets are smaller so they break up faster and penetrate less. For this reason the penetration curves of both cases are very similar.

The influence of the back (chamber) pressure is shown on Figure 8b. The higher density of the gas in the case of high pressures promotes the interaction between both phases, leading to lower penetration values. In addition to that, the released energy by the collapse of cavitation bubbles increases with high back pressures following the Rayleigh-Plesset equation [4]. Therefore the available breakup energy is higher for higher back pressures. This leads to a smaller mean droplet size calculated by the model for high back pressures, but only in the case of cavitating nozzles, as seen in Fig. 8d. This is also in agreement with the reports found in the literature dealing with the influence of the back pressure on the spray characteristics [14].

According to the empirical correlations found in the literature, the effect of the back pressure on the penetration length is at least so important as the effect of the injection pressure [14]. For the presented model the back pressure seems to have a clearly more significant effect than the injection pressure, what can be appreciated by comparing the difference between the calculated penetration lengths in Fig. 8a and 8b. Similar behaviour can be found when considering the mean droplet size of Figures 8c and 8d. Most of the empirical correlations for the droplet size distribution of the spray assume a similar effect of both injection and back pressures. The results of the simulation show a much higher effect of the injection pressure on the droplet size distribution. Here, it has to be considered that the empirical correlations were obtained considering both primary and secondary droplets and the diagrams of Figures 8c and 8d show only the mean size of the primary droplets, where reliable experimental data are very rare.

Figure 8e and 8f show the calculated near and far spray angles of the investigated nozzle compared to the measurements. The diagrams show also the influence of the back pressure on the development of the spray. The influence of the injection pressure is not represented because it does not play a role on the development of the spray angles, as derived from several empirical correlations developed for Diesel injection found in the literature [14, 13]. Both measurements and simulations show higher values in the case of high back pressures for both far and near angles. There are two main reasons for this behaviour: On the one hand, a bigger divergence of the droplets can be expected for higher back pressures due to the stronger interaction between gas and liquid. On the other hand, the released energy from bubble collapse depends on the back pressure, influencing the cavitation induced breakup energy, so that high energy levels lead to high radial velocities of the created droplets. Both effects influence the measured and calculated spray angles, as seen in Fig 8e-8f. The agreement between experiments and calculations is quite good for the near spray angles and reasonably good in the case of the far spray angles. Nevertheless, tendencies are well reproduced in both cases. This disagreement is due to the different division of the spray in three parts depending on the mass content (see Fig.7) for simulations and experiments, since in the latter case this information is obteined from a 2D picture, leading to slightly different results.

The diagrams of figures 8c and 8d show the mean size of the 300 parcels injected in the domain in every timestep. These

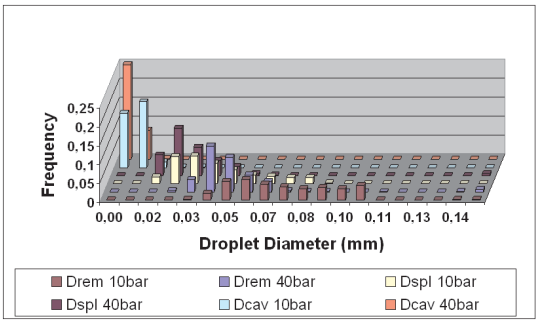

Figure 9: Primary Droplet Distribution for two different back pressures

values are calculated by the primary breakup model. The model calculates three different primary droplet sizes for every timestep depending on the origin of the breakup energy, d_{rem}, d_{spl}, d_{cav}. For a better description of the performance of the model, figure 9 shows a histogram of the frequency of the calculated sizes. As explained above, the size of the primary droplets for high chamber pressures is small because of the higher available breakup energies. In the histogram there is a shift to the left (lower sizes) for each of the three primary droplet types when increasing back pressure, following the trends found in experimental works [14]. On top of that, the calculated sizes for d_{cav}, which are the droplets to be found on the spray contour, are in very good agreement with the measured values by [8]. Droplets which are responsible of the far characteristics of the spray and correspond to the spray core (d_{rem}, d_{spl}) show sizes of about 30%-70% of the nozzle diameter, which are also plausible values for a cavitating nozzle under fully open needle conditions.

CONCLUSIONS

This paper has been focused on high-pressure-driven Diesel fuel spray simulation and a primary breakup model has been evaluated by means of optical measurements of a spray.

In order to take into account the flow conditions inside the nozzle on liquid jet breakup, a coupled approach has been used, including unsteady two phase 3D simulations of both nozzle flow and spray.

Unsteady nozzle flow simulations including opening injector needle have been carried out and compared with hydraulic measurements with satisfactory results.

Regarding the spray, the comparison between numerical results and experiments has shown the reasonably good performance of the presented model in predicting the primary breakup process, taking into account the shortcomings of the Lagrangian approach for the simulation of such two phase flows. In the area near the nozzle exit, right after the primary breakup takes place, measurements and simulations show a very good agreement. The initial penetration of the Diesel spray and its near angle are well predicted. On the contrary, penetration and spray angle of the spray in the far field of the nozzle show less good agreement due to the known mesh dependency of the Lagrangian approach and to the lack of coalescence model. It is important to note that even if the quantitative results are not as good as expected, the qualitative evaluation of the model predicts the right tendencies. Better quantitative results could be achieved with a lower value

of the constant C (Eq. 12), which would lead to bigger primary droplets and higher penetration.
These results, and others which will be published in the near future, show that the presented primary breakup model is a very good starting point in order to understand and describe the influence of the nozzle flow on the primary breakup. On the other hand, this investigation also showed the suitability of the Lagrangian approach for the simulation of the thin spray, while an Eulerian approach could be more efficient for the calculation of dense sprays.

NOMENCLATURE

Symbol	Quantity	Unit
CCP	Critical Cavitation Point	bar
CF	Conicity Factor	-
d	Droplet Diameters	m
D	Nozzle Diameters	m
E	Energy	$Kg \cdot m^2/s^2$
L	Length	m
m	Mass	Kg
HD	Hydraulic Flow	l/s
HE	Inlet Rounding	m
p	Pressure	bar
S_p	Penetration	m
t	Time	s
VF	Volume Fraction	-

Greek Letters

Γ_{disp}	Mesh Stiffness	N/m
δ	Nodes displacement	m
η	Efficiency	-
σ	Surface Tension	N/m
μ	Dynamic Viscosity	$Kg/m \cdot s$

Subscripts

1	Liquid Zone
2	Cavitation Zone
ber	Bernouilli
cav	Cavitation
eff	Effective
exp	Experiment
geg	After Nozzle
in	Inlet
inj	Injection
kin	Kinetic
L	Liquid
out	Outlet
r	Radial
rem	Remaining Mass
sim	Simulation
spl	Split Mass
turb	Turbulence
vor	Before Nozze

References

[1] *ANSYS CFX-Solver Theory Guide*. Ansys Europe, Ltd., 2006.

[2] C. Arcoumanis and M. Gavaises. Linking nozzle flow with spray characteristics in a diesel fuel injection system. *Atomization and Sprays*, 8:307–347, 1998.

[3] C. Baumgarten. *Modellierung des Kavitationseinflusses auf den primären Strahlzerfall bei der Hochdruck-Dieseleinspritzung*. PhD thesis, University Hannover, 2003.

[4] C.E. Brennen. *Cavitation and Bubble Dynamics*. ISBN 0-19-509409. Oxford University Press, 1995.

[5] R. Busch. *Untersuchung von Kavitationsphänomenen in Dieseleinspritzdüsen*. PhD thesis, University Hannover, 2001.

[6] H. Chaves, M. Knapp, A. Kubitzek, F. Obermeier, and T. Schneider. Experimental study of cavitation in the nozzle hole of diesel injectors using transparent nozzles. *SAE*, (SAE 950290), 1995.

[7] N. Chigier and R.D. Reitz. Regimes of jet breakup and breakup mechanisms (physical aspects). *Recent Advances in Spray Combustion: Spray Atomization and Drop Burning Phenomena*, 1, 1996.

[8] A. Fath. *Charakterisierung des Strahlaufbruch-Prozesses bei der instationären Druckzerstäubung*. PhD thesis, Universität Erlangen-Nürnberg, 1997.

[9] E. Kull. *Einfluss der Geometrie des Spritzlochs von Dieseleinspritzdüsen auf das Einspritzverhalten*. PhD thesis, Universität Erlangen-Nürnberg, 2003.

[10] E. Kumzerova. Validation of spray simulations in cfx-11. *Ansys CFX Internal Validation Report*, 2006.

[11] A. Nishimura and D.N. Assanis. A model for primary diesel fuel atomization based on cavitation bubble collapse energy. *Institute for Liquid Atomization and Spray Systems*, 2000.

[12] P. Pelloni and G.M. Bianchi. A cavitation-induced atomization model for high-preesure diesel spray simulations. *32 ISATA International Congress*, (99SIO44), 1999.

[13] R.D. Reitz and F.V. Bracco. Mechanisms of atomization of a liquid jet. *Phys. Fluids*, 1982.

[14] B.M. Schneider. *Experimentelle Untersuchungen zur Spraystruktur in transienten, verdampfenden und nicht verdampfenden Brennstroffstrahlen unter Hochdruck*. PhD thesis, Eidgenössischen Technischen Hochschule Zürich, 2003.

[15] M. Sommerfeld. *Modellierung und numerische Berechnung von Partikelbeladenen Strömungen mit Hilfe des Euler/Lagrange-Verfahrens*. Shaker Verlag, Aachen, 1996.

[16] F.X. Tanner. A cascade atomization and drop breakup model for the simulation of high-pressure liquid jets. *SAE*, (2003-01-1044), 2003.

[17] E. von Berg, A. Alajbegovic, D. Greif, A. Poredos, R. Tatschl, E. Winklhofer, and L.C. Ganippa. Primary break-up model for diesel jets based on locally resolved flow field in the injection hole. *Institute for Liquid Atomization and Spray Systems*, 2002.

[18] E. von Berg, W. Edelbauer, A. Alajbegovic, R. Tatschl, M. Volmajer, B. Kegl, and L.C. Ganippa. Coupled simulations of nozzle flow, primary fuel jet breakup, and spray formation. *Journal of Engineering for Gas Turbines and Power*, Vol 127:897, 2005.